UCRL-JC-122411
PREPRINT
CONF-9510223--2

X-ray Laser Interferometry: A New Tool for AGEX (U)

Alan S. Wan, Juan C. Moreno, Stephen B. Libby, Robert Cauble,
Troy W. Barbee, Jr., Peter Celliers, Luiz D. Da Silva,
Richard A. London, James E. Trebes, Franz Weber
Lawrence Livermore National Laboratory
Livermore, CA 94550

This paper was prepared for submittal to the
Tenth Biennial Nuclear Explosives Design
Physics Conference (NEDPC),
Los Alamos, NM
October 30 - November 3, 1995

October 1995

X-ray Laser Interferometry: A New Tool for AGEX (U)

Alan S. Wan, Juan C. Moreno, Stephen B. Libby, Robert Cauble, Troy W. Barbee, Jr., Peter Celliers, Luiz B. Da Silva, Richard A. London, James E. Trebes, Franz Weber
Lawrence Livermore National Laboratory

Collisionally pumped soft x-ray lasers now operate over a wavelength range extending from 4 - 40 nm. With the recent advances in the development of multilayer mirrors and beamsplitters in the soft x-ray regime, we can utilize the unique properties of x-ray lasers to study large, rapidly evolving laser-driven plasmas with high electron densities. By employing a shorter wavelength x-ray laser, as compared to using conventional optical laser as the probe source, we can access a much higher density regime while reducing refractive effects which limit the spatial resolution and data interpretation. Using a neon-like yttrium x-ray laser which operates at a wavelength of 15.5 nm, we have performed a series of soft x-ray laser interferometry experiments, operated in the skewed Mach-Zehnder configuration, to characterize plasmas relevant to both weapons and inertial confinement fusion. The two-dimensional density profiles obtained from the interferograms allow us to validate and benchmark our numerical models used to study the physics in the high-energy density regime , relevant to both weapons and inertial confinement fusion. (U)

Introduction

Since the first demonstration of a soft x-ray laser,[1,2] x-ray lasers have been considered for applications in the fields of microscopy, holography, material science, and plasma physics.[3] With its short wavelength (4–40 nm), short controllable pulse duration, high peak brightness, and sufficient spatial and temporal coherence, the x-ray laser is ideally suited as a plasma diagnostic to image rapidly evolving (< 1 ns) laser-driven plasmas with high electron densities (10^{21} cm^{-3} < n_e < 10^{24} cm^{-3}).

With recent advances in the development of short wavelength multilayer mirrors and beamsplitters in the soft x-ray regime,[4] we are pioneering the development and applications of x-ray lasers as imaging diagnostics for laser plasmas. Using x-ray lasers as high fluency monochromatic radiographic sources, radiographic images of smooth laser accelerated foils have shown small-scale (~10 μm) filamentation which may reveal limitations for direct-drive inertial confinement fusion (ICF) capsules due to unexpectedly intense hydrodynamic instabilities.[5] We have also used x-ray lasers to measure 1-D density gradients of laser plasmas using the Moiré deflectometry technique.[6]

This paper is focused on the application of x-ray lasers to obtaining absolute measurements of electron density using a soft x-ray laser interferometer. Extending conventional interferometric techniques into the soft x-ray range has been difficult because of the problems with designing optical systems which operate in the range 4-40 nm. Fortunately, multilayer mirror technology has now evolved to the point where artificial structures can be routinely fabricated with reflectivities as high as 65% at 13 nm,[7,8] and with the overall uniformities required by more conventional interferometers. We have also successfully fabricated large active area (1.2 cm x 1.2 cm) beamsplitters with excellent reflectivity and transmission at short wavelengths. The flatness of the beamsplitters was measured with an optical interferometer; over the clear aperture the flatness was typically better than 500 nm for high quality silicon substrates. Utilizing these multilayer optical components and a collisionally pumped neon-like yttrium x-ray laser operating at 15.5 nm as the probe source, we have successfully demonstrated a soft x-ray laser interferometer in a skewed Mach-Zehnder configuration.

The applicability of the soft x-ray laser interferometry technique to study the physics of laser-produced plasmas is the primary focus of this paper. Detailed comparisons of absolute two-dimensional electron density profiles obtained from x-ray laser interferograms and profiles obtained from radiation hydrodynamics codes, such as LASNEX, will allow us to validate and benchmark complex numerical models used to study the physics of laser-plasma interactions. Thus the development of x-ray laser interferometry technique provides a mechanism to probe the deficiencies of our numerical models and is an important tool for the high-energy density physics and science-based stockpile stewardship programs. In section 2 we describe the setup of the soft x-ray laser interferometer at 15.5 nm using a yttrium x-ray laser. We have

measured electron densities exceeding 1 x 10^{21} cm^{-3} in a colliding plasma configuration which is millimeters in extent and we will present that result in section 3. In section 4 we discuss issues that are relevant to data analysis. We summarize and outline our future research direction in section 5.

Experimental Setup

Accessible regime of a soft x-ray laser interferometer

To obtain accurate and absolute measurements of electron density profiles for high density, laser-produced plasmas, optical interferometry was used to study exploding foils for x-ray laser dynamics,[9,10,11] to examine profile steepening due to radiation pressure,[12] and to study filamentation instabilities.[13,14] However, the size and density regime of the laser plasma accessible to an optical interferometer are limited by inverse bremsstrahlung absorption and refractive propagation of probe beams facing large density gradients. By employing a shorter wavelength x-ray laser, we can access a much higher density regime while reducing refractive effects which limit the spatial resolution and data interpretation.

In a plasma, the index of refraction, n_{ref}, is related to the critical electron density, n_{cr} = 1.1 x 10^{21} λ^{-2} [cm^{-3}] (λ is the wavelength of the probe laser in μm), by $n_{ref} = \sqrt{1 - n_e/n_{cr}}$. In an interferometer the number of fringe shifts, N_{Fringe}, is then given by

$$N_{Fringe} = \frac{\delta\phi}{2\pi} = \frac{1}{\lambda}\int_0^L (1 - n_{ref})\, dl \approx \frac{n_e}{2n_{cr}}\frac{L}{\lambda}, \qquad (1)$$

where L [μm] is the path length across the target plasma and we assume refraction effects are negligible. Experimentally the maximum number of fringe shifts measurable is usually constrained by detector resolution and is rarely greater than ~50. This imposes a constraint on the product n_eL for a given wavelength.

An additional constraint which limits the accessible density and length parameter space is absorption. In a plasma dominated by free-free absorption the absorption coefficient, α (in units of cm^{-1}), is approximately given by[15]

$$\alpha \approx 2.44\times10^{-37}\,\frac{\langle Z^2\rangle\, n_e\, n_i}{\sqrt{kT}\,(h\nu)^3}\left[1 - \exp\left(\frac{-h\nu}{kT}\right)\right], \qquad (2)$$

where the electron temperature, kT, and photon energy, $h\nu$, are in eV and electron and ion densities are in cm^{-3}. The strong scaling with photon energy shows the advantage of probing with soft x-ray sources. For most high temperature plasmas of interest, the level of ionization is sufficient to eliminate any bound-free absorption in the soft x-ray region. Resonant line absorption is possible but very unlikely given the narrow bandwidth of the x-ray laser, ~0.001 nm.[16] Therefore, if we consider only free-free absorption in a plasma with 1 keV temperature and average ionization of 30 (mid-Z plasma) we obtain from Eqn. 2, $\alpha \approx 2.6\times10^{-43} n_e^2$. If we allow for one optical depth (i.e. $\alpha L = 1$) of absorption we obtain $n_e^2 L = 3.8\times10^{42}$. In Figure 1 the shaded region represents the electron density and plasma dimension accessible with a soft x-ray laser source (15.5 nm) which is constrained by free-free absorption and a maximum of 50 fringe shifts. This parameter space easily covers plasmas normally produced in the laboratory.

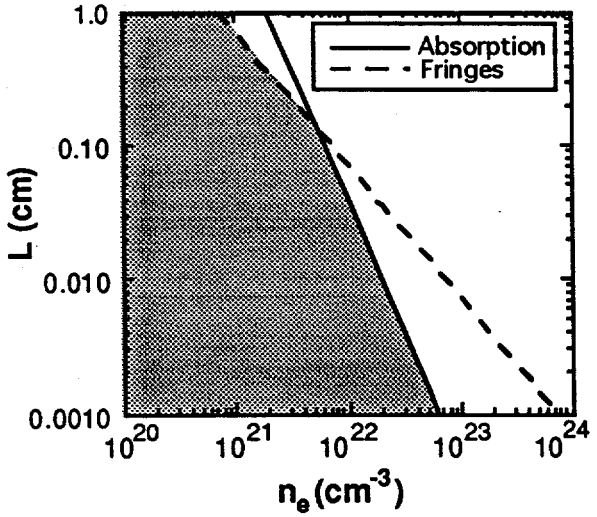

Figure 1. The shaded portion represents the regime of electron density and plasma dimension accessible with a soft x-ray laser source (15.5 nm) which is constrained by free-free absorption and a maximum of 50 fringe shifts.

Experimental setup

The experimental setup used to probe plasmas is shown schematically in Figure 2. The system consists of a collimated x-ray laser source, an imaging mirror and an interferometer. For our experiments we chose to construct a skewed Mach-Zehnder interferometer consisting of two flat multilayer mirrors and two multilayer beamsplitters, presenting a near-normal angle of incidence between beam and multilayer components. The polarizing properties of multilayer mirrors when operated at 45 degrees prevented us from using a more conventional Mach-Zehnder geometry. In order to

reduce background self-emission, a series of three multilayer mirrors were used prior to the CCD detector, reducing the bandpass of the system. The effective bandpass of this system was 0.4 nm, which is significantly broader than the 0.001 nm spectral width of the x-ray laser source. The image magnification was 19 giving a pixel limited resolution of ~1.3 μm. Reference 17 gives a detailed description of the instrumentation and the multilayer components.

The transmissive and reflective properties of the multilayer components, at the appropriate wavelength and operating angles, were characterized prior to the experiment. The multilayer mirrors have a peak reflectivity of 60±5% at 15.5 nm. The beamsplitters used in the interferometer are the most critical element of the system. The measured reflectivity and transmission for these beamsplitters at 15.5 nm were 20% and 15% respectively. The overall throughput of each arm, accounting for the mirror and beamsplitter (one transmission & one reflection), was ~ 0.6 x 0.20 x 0.15 = 18%.

A collisionally pumped neon-like yttrium x-ray laser operating at 15.5 nm was used as the probe source. The x-ray laser was produced by irradiating a solid 3-cm-long yttrium target with one beam from Nova (λ_{laser} = 0.53 μm, 600-ps-long, temporally square) at an intensity of 1.5×10^{14} W/cm^2. The x-ray laser has an output energy of 3±2 mJ, a divergence of approximately 10-15 mrad (FWHM) and an output pulse width of 350 ps. The short pulse and high brightness of the x-ray laser allowed us to obtain an interferogram in a single 350 ps exposure thereby reducing the effects of vibrations and motion blurring. The timing between the two Nova lasers, one to generate the x-ray laser and one to produce the target laser plasma, was defined by the time-of-flight path of our interferometer setup and the desired probe time. Reference 18 describes the measurement of the transverse and temporal coherence properties of the x-ray laser which are important in the design of our interferometer.

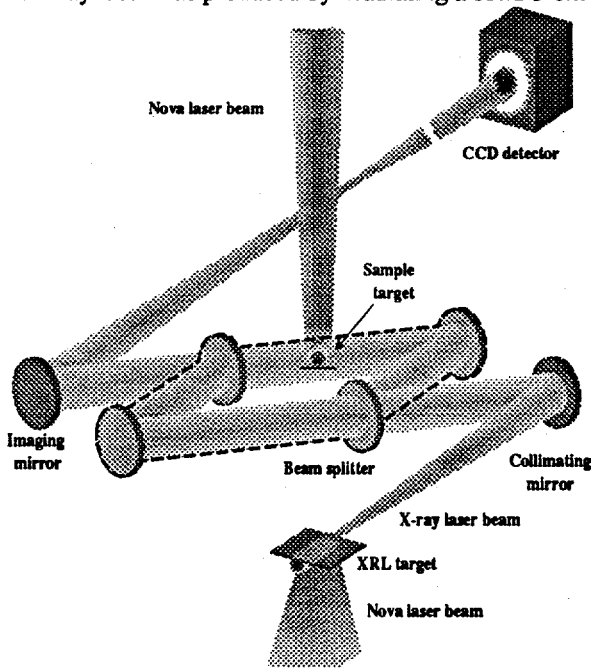

Figure 2. Experimental setup of the soft x-ray laser interferometer system which consists of a collimated x-ray laser source (formed at the bottom with the collimating mirror), an interferometer in a skewed Mach-Zehnder configuration (shown with dashed outline) with the sample target irradiated by another Nova laser beam (coming from the top), and an imaging mirror.

Colliding Plasma Experimental Setup and Results

The soft x-ray laser interferometry technique was first demonstrated on the Nova 2-beam during July 1994.[17,19] Since then we have used this technique to study various targets, including exploding foils[20] and plastic (CH) disks.[17,19] We are currently installing cylindrical lenses on the Nova 10-beam facility in order to field x-ray laser experiments there with the goal of ultimately measuring the 2-D density profiles of a hohlraum.[21]

We have recently begun a set of experiments designed to study the collision of high-density, high-temperature plasmas. Significant wall blowoff in vacuum hohlraum targets for the next generation ICF machines, such as the National Ignition Facility (NIF), can result in plasma colliding on-axis. The stagnation of plasma on-axis can result in jets streaming toward the capsule and destroy the capsule symmetry and degrading the ICF capsule yield. One alternative to this problem is to use a gas-filled hohlraum. However, the addition of the fill gas introduces problems in laser absorption, refraction, and instabilities.[22]

The setup of our first colliding plasma experiment is shown in Figure 3. Since we only have 2 beams available to us in this first generation x-ray laser interferometer, and one beam must be devoted to generate the x-ray laser, we need to design a colliding plasma configuration using the one remaining laser beam. We chose to orient two slanted gold slabs at 45° with respect to the axis of symmetry. The minimum gap between the two slabs is 500 μm in this experiment. We generate a 500 μm full-width (FW) line-focused laser beam which incidents the slabs, as shown in Fig. 3, and generates plasmas blowing toward each other. The laser has an intensity on target of

$3x10^{14}$ W/cm^2 and has a 1-ns squared temporal pulse shape. At late time the plasma collides on-axis. We expect to observe a varying degree of stagnation with the strongest effect near the minimum gap region.

The target was backlit edge-on by the x-ray laser beam 1.0 ns after the start of the laser pulse that generated the gold plasma. The collimated x-ray laser beam was several millimeters in extend and was directed parallel to the *z*-axis. The side view of Fig. 3 shows the view in the direction of the x-ray laser probe beam. The CCD has a 500-ps gate and is set to centered with respect to the x-ray laser pulse.

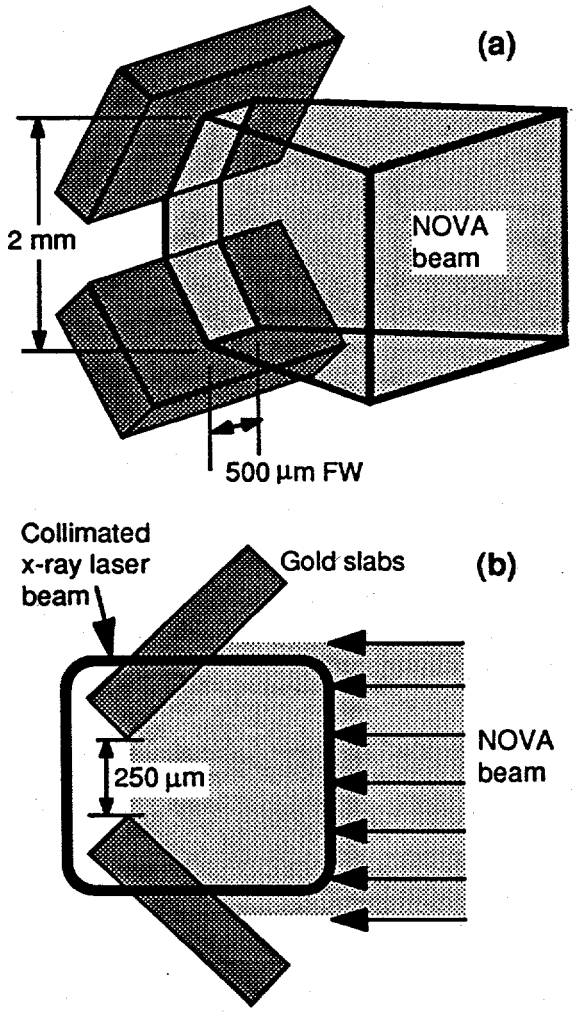

Figure 3. Experimental configuration for the colliding plasma experiment. (a) 3-D view of the Nova beam illuminating the 2 gold slabs oriented at 45 degrees w.r.t. the axis of symmetry. (b) side view showing the window of collimated x-ray laser beam which defines the view of the CCD camera.

In Fig. 4 we show the measured interferogram of the colliding plasma, in the geometry defined by the side view of Fig. 3. The image shows excellent fringe visibility. The visibility is poorer at the right hand edge of the interferogram due to slight miss-timing in the gated CCD setup. We also observed significant self emission from the plasma near the slab surface. We can further reduce the self emission by better optical quality of the system by reducing the bandpass near the x-ray laser wavelength and by better gating of the CCD detector.

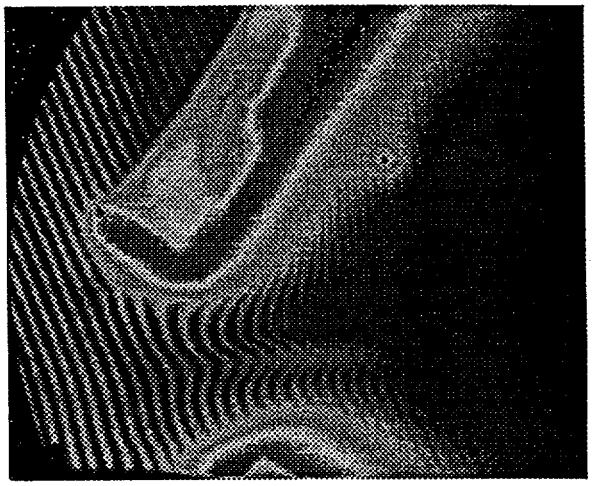

Figure 4. Measured interferogram of the colliding plasma. We observed excellent fringe visibility with strong self emission near the slab surface. Large fringe shifts on-axis is evident due to stagnation of the plasma in the colliding geometry. Null fringes are visible to the left of the slabs.

Near the symmetry axis between the two gold slabs we can clearly observe significantly greater fringe shifts as the results of the plasma stagnation due to the plasma collision. At the extreme left and right of the interferogram shown in Fig. 4 we can still see the unperturbed fringe pattern where there is no plasma. We can use these unperturbed fringes to reconstruct a unperturbed fringe mapping for the entire coverage. We can then use that reconstructed mapping as a reference to measure the amount of fringe shift due to the presence of the plasma. The beamsplitters were not perfectly flat, creating some minor variations in the unperturbed fringe pattern and that is one of our dominant experimental uncertainties. Based on previous null shots with similar quality beamsplitters, we estimate the uncertainty to be of order 0.1 fringe. Another uncertainty is the determination of the plasma path length. Reference 19 addresses the uncertainties of the path length due to 3-D plasma expansion and how that might affect our data interpretation. In this paper we will use the 500 μm FW as the path length.

Data Analysis

We use IDL (Interactive Data Language) to process the interferogram and analyze the data in 2-D. Figure 5 shows an overlay of the measured fringes, shown in solid lines, and a 2-D mapping of the unperturbed fringes, shown in dotted lines. The unperturbed, or null fringes, are obtained using the measured fringes at the perimeter of the interferogram where we little or no plasma. We can then project a 2-D mapping of this unperturbed fringe, from which we can obtain a local fringe shift.

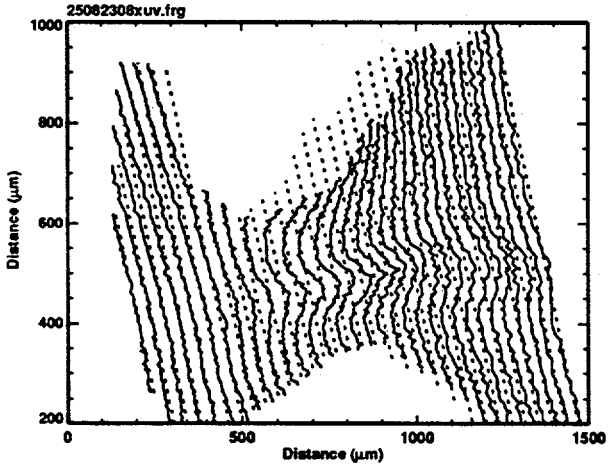

Figure 5. 2-D mapping of the measured fringes (solid lines) and projected null fringes (dotted lines)

The measured fringe shift can be translated directly to a local n_e value according to Eqn. (1). The only uncertainty is the path length, L, across the target plasma in the direction of the collimated x-ray laser beam. This can be a significant uncertainty since plasma expands in 3-D. Since we presently have no 3-D code available to properly estimate the 3-D effect, in this paper we assume a uniform plasma with a 500 μm path length. However, we are working on a fully 3-D radiative hydrodynamics code[23] which may be able to simulate our geometry.

Figure 6 shows the measured 2-D n_e profile in the colliding geometry. Here we observed significant density increase on-axis due to the collision. Measured n_e is as high as 8 x 10^{20} cm^{-3}, which is a factor of 3-4 higher than the estimated n_e value without collision. The stagnation region is both wide, of order 600 μm, and thick, of order 100 μm. The thickness of this stagnation region may indicate a significant degree of plasma interpenetration, which would deviate from a pure fluid-like behavior.

LASNEX,[24] which we primarily use to simulate large scale, multi-dimensional laser plasma

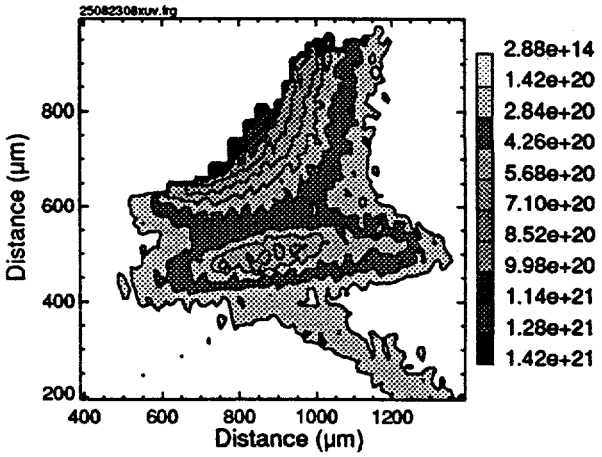

Figure 6. Measured 2-D n_e profile, assuming a uniform plasma with path length of 500 μm. At the symmetry axis we observed significant density increase due to plasma stagnation. n_e value on-axis is as high as 8 x 10^{20} cm^{-3}, which is a factor of 3-4 higher than the estimated n_e value without collision.

experiments, includes many physics models necessary to simulate a multi-dimensional radiative hydrodynamics problem, including laser-matter interaction, radiation transfer, electron thermal diffusion by conduction, and simple description of non-local thermodynamic equilibrium atomic kinetics. By specifying the modeling geometry and laser configurations, such as those shown in Fig. 3, and physics parameters, such as the electron flux-limited multiplier, and electron-ion coupling, LASNEX self-consistently calculates the evolution of the laser-produced plasma base on laser energy deposition, atomic kinetics, and radiation hydrodynamics. The output of these calculations include plasma parameters such as electron and ion temperatures and densities, which we can use to compare against measurements such as the spatial n_e profile derived from x-ray laser interferometry.

A strong motivation to do the colliding plasma experiment is to examine the validity of LASNEX, which is a Lagrangian fluid code, in a regime that might deviate from the fluid behavior. We are currently simulating this colliding plasma experiment using LASNEX, and compare the LASNEX output with the output of a multi-specie PIC code,[25,26] which should better predict the interpenetration of the plasma. It is the validity and benchmarking of these numerical models, with the absolute n_e measurements at high densities, that are the primary reasons for performing experiments using x-ray laser interferometry.

Summary

The results presented in this paper illustrate the important role soft x-ray laser interferometry can play in diagnosing laser produced plasmas. We have demonstrated that using a soft x-ray laser interferometer we have measured n_e profiles that exceed 10^{21} cm^{-3} for a large plasma that is millimeters in extent. The measured fringe visibility is very good. Using narrow bandwidth multilayer optics, we observed very little self emission from the plasma, except for the region right at the slab surface.

We have used the x-ray laser interferometer to study colliding plasmas. The collision of the laser-produced plasmas, generated from gold slabs oriented at 45° from the symmetry axis, results in significant density increase due to plasma stagnation. We are currently analyzing data using both LASNEX and a PIC code.

The ultimate motivation of the development of x-ray laser interferometry is to provide a mechanism to probe the deficiencies of our numerical model in areas such as laser deposition by both resonance and inverse bremsstrahlung absorption, flux-limited heat conduction, hydrodynamics, and non-local thermodynamics equilibrium atomic kinetics. The validation and benchmarking of the codes will allow us to gain better understanding of the physics of high-density laser-produced plasmas as we design more and more complex laser experiments for studying weapon physics, and hohlraum and capsules for ICF applications. Because of its unique potential, the development of x-ray laser imaging diagnostics represents an important step in our development of tools for above ground experiments on both present and future laser facilities.

Acknowledgments

This work was performed under the auspices of the U. S. DOE by LLNL under the contract number W-7405-ENG-48 and is partially supported by the Institute Sponsored Research Program.

References

1. D. Matthews, P. L. Hagelstein, M. D. Rosen, M. J. Eckart, et al., *Phys. Rev. Lett.*, **54**, 110 (1985).
2. S. Suckewer, C. H. Skinner, H. Milchberg, C. Keane, D. Voorhees, *Phys. Rev. Lett.*, **55**, 1753 (1985); S. Suckewer, C. H. Skinner, D. Kim, et al., *Phys. Rev. Lett.*, **57**, 1004 (1986).
3. *Proceeding of the Applications of X-ray Lasers Workshop*, R. A. London, D. L. Matthews, and S. Suckewer, ed., Report CONF-9206170, Lawrence Livermore National Laboratory (January 1992).
4. E. Spiller, Soft X-ray Optics (SPIE, Bellingham, WA, 1994).
5. R. Cauble, L. B. Da Silva, T. W. Barbee, Jr., P. Celliers, et al., *Phys. Rev. Lett.*, **74**, 3816 (1995).
6. D. Ress, L. B. Da Silva, R. A. London, J. E. Trebes, et al., *Science*, **265**, 514 (1994).
7. T. W. Barbee Jr., J. C. Rife, W. R. Hunter, M. P. Kowalski, et al., *Appl. Opt.*, **32**, 4852 (1993).
8. D. G. Stearns, R. S. Rosen, and S. P. Vernon, *J. Vac. Sci. Technol. A, Vac. Surf. Films*, **9**, 2662–2669 (1991).
9. M. Rosen, P. L. Hagelstein, D. L. Matthews, E. M. Campbell, et al., *Phys. Rev. Lett.*, **54**, (1985).
10. G. Charatis, G. E. Busch, C. L. Shepard, P. M. Campbell, and M. D. Rosen, *J. de Physique*, **C6**, 89-98 (1986).
11. M. K. Prasad, K. G. Estabrook, J. A. Harte, R. S. Craxton, et al., *Phys. Fluids B*, **4**, 1569 (1992).
12. D. T. Attwood, D. W. Sweeney, J. M. Auerbach, and P. H. Y. Lee, *Phys. Rev. Lett.*, **40**, 184 (1978).
13. P. E. Young, *Phys. Fluids B*, **3**, 2331 (1991).
14. S. Wilks, P. E. Young, J. Hammer, M. Tabak, and W. L. Kruer, *Phys. Rev. Lett.*, **73**, 2994–2997 (1994).
15. C. W. Allen, *Astrophysical Quantities*, p. 100 (Oxford University Press, New York, 1963).
16. J. Koch, B. J. MacGowan, L. B. D. Silva, D. L. Matthews, et al., *Phys. Rev. Lett.*, **68**, 3291 (1992).
17. L. B. Da Silva, T. W. Barbee, Jr., R. Cauble, P. Celliers, et al., *Phys. Rev. Lett.*, **74**, 3991 (1995).
18. P. Celliers, F. Weber, L. B. Da Silva, T. W. Barbee, Jr., et al., *Opt. Lett.*, **20**, 1907 (1995).
19. A. S. Wan, L. B. Da Silva, T. W. Barbee, Jr., R. Cauble, et al., "Application of X-Ray Laser Interferometry to Study High-denisty Laser-produced Plasmas," to be published in *Journal of Optical Society of America B: Optical Physics*

20. A. S. Wan, L. B. Da Silva, T. W. Barbee, Jr., R. Cauble, et al., "X-ray Laser Interferometry for Probing High-density Plasmas," in "Soft X-ray Lasers and Applications," J. Rocca and P. L. Hagelstein, editors, SPIE Annual Conference 1995, 9-14 July, 1995, San Diego.
21. R. A. London, C. Decker, L. Powers, J. A. Harte, et al., "Design and Analysis of X-ray Laser Probing Experiments of Laser-Fusion Plasmas," in "Soft X-ray Lasers and Applications," J. Rocca and P. L. Hagelstein, editors, SPIE Annual Conference 1995, 9-14 July, 1995, San Diego.
22. S. W. Haan, S. M. Pollaine, J. D. Lindl, L. J. Suter, et al., Phys. Plasmas, 2, 2480–2487 (1995).
23. D. S. Kershaw, M. K. Prasad, M. J. Shaw, "Three-dimensional Unstructured-mesh Eulerian Hydrodynamics with the Upwind Discontinuous Finite Element Method," to be submitted to *J. Comput. Phys.*, (1995).
24. G. B. Zimmerman and W. L. Kruer, *Com. Plasma Phys. and Cont. Fusion*, 2, 51 (1975).
25. P. W. Rambo, J. Denavit, *Phys. Plasmas*, 1, 4050–4060 (1994).
26. P. W. Rambo, R. J. Procassini, *Phys. Plasmas*, 2, 3130–3145 (1995).